

Electronic Supplementary Information (ESI) available for:

**Cation non-stoichiometry in multi-component oxide nanoparticles by solution chemistry: A case study on CaWO<sub>4</sub> for tailored structural properties**

5

**Wanbiao Hu, Wenming Tong, Liping Li, Jing Zheng, and Guangshe Li\***

*State Key Laboratory of Structural Chemistry, Fujian Institute of Research on the Structure of Matter and Graduate School of Chinese Academy of Sciences, Fuzhou 350002 (P. R. China)*

10

*E-mail: guangshe@fjirsm.ac.cn*

**Supporting Online Materials**

15 **Table S1.** Elemental analysis before and after Ar<sup>+</sup> ion bombarding on the as-prepared CaWO<sub>4</sub> nanocrystals using XPS.

**Fig. S1.** XRD patterns of Zn<sup>2+</sup> doped CaWO<sub>4</sub> samples with varied initial doping level of Zn<sup>2+</sup> comparing with un-doped sample.

20 **Fig. S2.** TEM and HRTEM images of Zn<sup>2+</sup> doped CaWO<sub>4</sub> nanocrystals with the initial molar ratio of Zn<sup>2+</sup>/(Ca<sup>2+</sup>+Zn<sup>2+</sup>) at 0.15.

**Fig. S3.** XRD patterns of the sample after firing the as-prepared Zn<sup>2+</sup> doped CaWO<sub>4</sub> nanocrystals at 800 °C in air for 2 h.

**Fig. S4.** Raman spectroscopy of the samples prepared with and without involving citric acid.

25 **Fig. S5.** High-resolution XPS spectra of O1s for Ca<sub>1-x</sub>Zn<sub>x</sub>WO<sub>4</sub> nanocrystals at given dopant contents.

**Fig. S6.** XRD patterns of the samples prepared with and without involving citric acid.

**Table S1.** Elemental analysis for the as-prepared CaWO<sub>4</sub> nanoparticles before and after Ar<sup>+</sup> ion bombarding using XPS.\*

Bombarding time (0 s)						
Name	Peak/BE	Height/CPS	FWHM/eV	Area/CPS.eV	At. %	Ca2p/W4f
<b>C1s</b>	284.62	10388.61	2.15	33914.4	32.19	<b>3.03</b>
<b>O1s</b>	530.59	57275.1	2.1	144247	48.97	
<b>W4f</b>	35.21	19648.59	1.39	49823.2	<b>4.68</b>	
<b>Ca2p</b>	346.95	26491.59	1.41	74909.71	<b>14.16</b>	

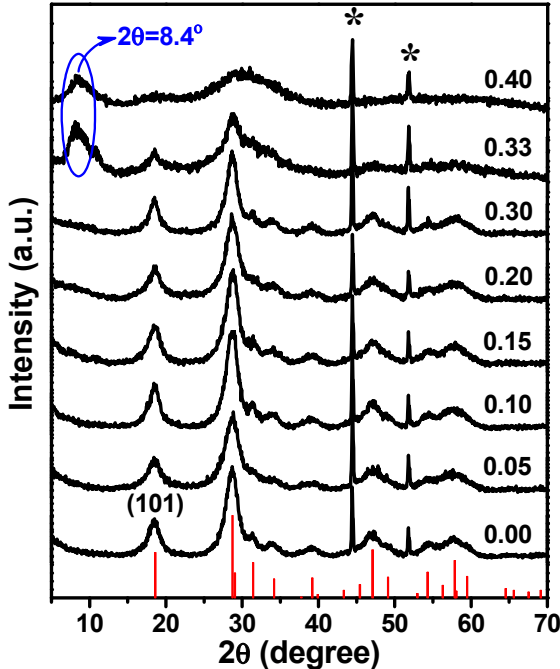
  

Bombarding time (5 s)						
Name	Peak/BE	Height/CPS	FWHM/eV	Area/CPS.eV	At. %	Ca2p/W4f
<b>C1s</b>	284.63	9502.31	1.85	30701.78	29.59	<b>2.97</b>
<b>O1s</b>	530.57	59949.68	1.99	147494.02	50.84	
<b>W4f</b>	35.29	20107.61	1.44	51755.83	<b>4.93</b>	
<b>Ca2p</b>	346.98	27521.94	1.57	76245.64	<b>14.64</b>	

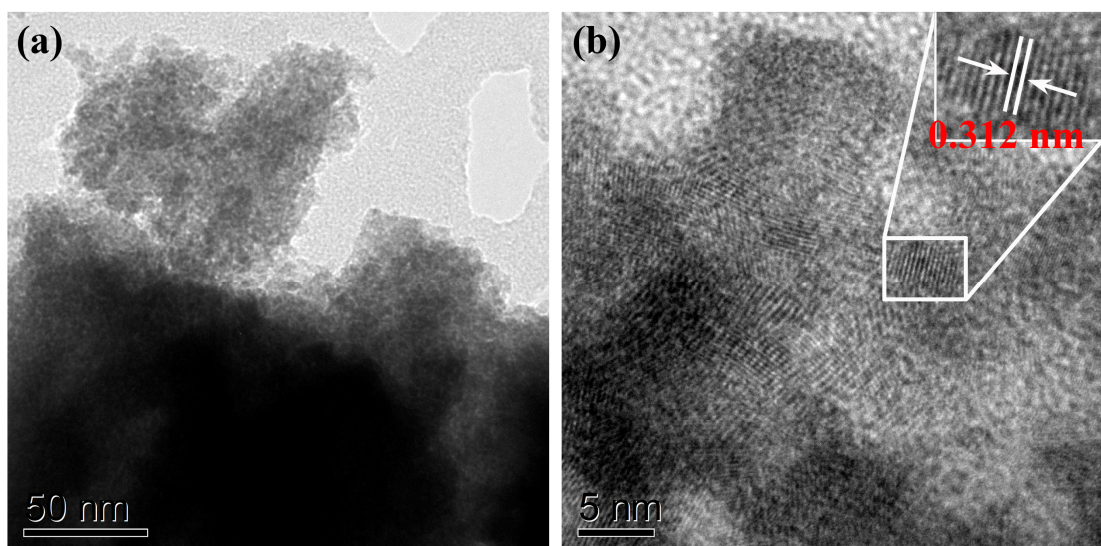
  

Bombarding time (10 s)						
Name	Peak/BE	Height/CPS	FWHM/eV	Area/CPS.eV	At. %	Ca2p/W4f
<b>C1s</b>	284.62	11277.79	1.75	34633.51	33.5	<b>2.91</b>
<b>O1s</b>	530.59	54037.56	2.16	141793.03	49.06	
<b>W4f</b>	35.21	18423.49	1.4	46609.84	<b>4.46</b>	
<b>Ca2p</b>	346.94	24909.52	1.52	67359.87	<b>12.98</b>	

\* From the above table, it is clear that the ratio of Ca2p/W4f was decreased after Ar<sup>+</sup> ion bombarding on the sample for once, i.e., 5 s, which was further decreased after the second bombarding, i.e., the bombarding of 10 s. This indicated that the excessive cation should occur on the nanoparticles' surfaces.



**Fig. S1.** XRD patterns of  $\text{CaWO}_4$  samples with varied initial doping level of  $\text{Zn}^{2+}$  comparing with undoped sample. The numbers denote the initial doping ratio of  $\text{Zn}^{2+}/(\text{Zn}^{2+}+\text{Ca}^{2+})$ . Vertical bars at the bottom denote the standard data for scheelite structure of bulk  $\text{CaWO}_4$  (JCPDS, No. 77-2233). Symbols “\*” denote the internal standard of Ni. It was found that when the ratio of  $\text{Zn}^{2+}$  was below 0.30, no traces of possible impurities like monoclinic wolframite-typed  $\text{ZnWO}_4$  or  $\text{ZnO}$  were observed. Doping  $\text{Zn}^{2+}$  did not lead to the width variations of diffraction peaks. Strong diffraction intensities of all samples characterized the high crystallinity. Using Scherrer formula, crystallite sizes of all samples were estimated to be around 6 nm from diffraction line (101). When the initial ratio of  $\text{Zn}^{2+}/(\text{Zn}^{2+}+\text{Ca}^{2+})$  was beyond 0.30, an impurity phase centered at  $2\theta=8.4^\circ$  appeared.



**Fig. S2.** TEM and HRTEM images of  $\text{CaWO}_4$  nanocrystals with an initial ratio of  $\text{Zn}^{2+}/(\text{Zn}^{2+}+\text{Ca}^{2+})$  at 0.15.

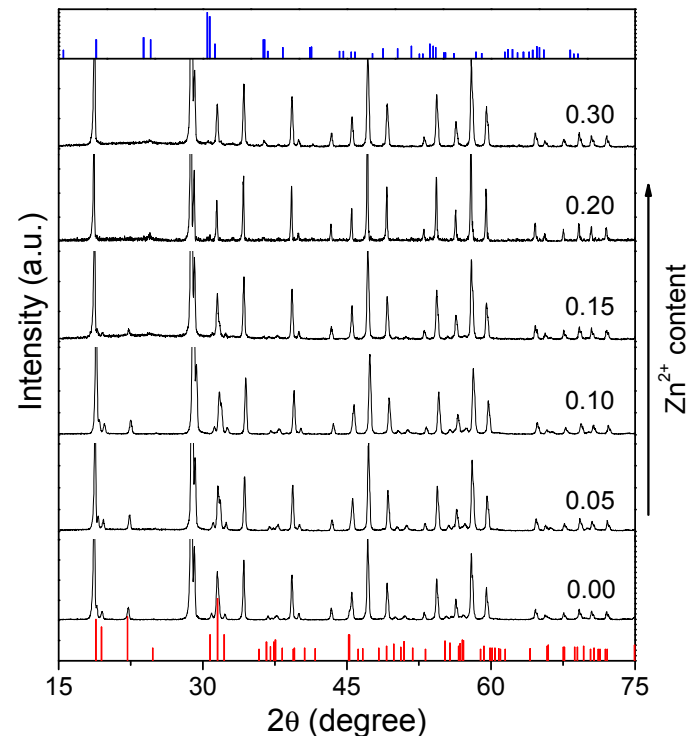


**Fig. S3.** XRD patterns of the samples after firing  $\text{CaWO}_4$  nanocrystals with given doping levels at 800 °C in air for 2 h. Vertical bars at the bottom and top denote the standard data for monoclinic  $\text{Ca}_3\text{WO}_6$  (S.G.: P2<sub>1</sub>/n; JCPDS No. 22-0541) and monoclinic wolframite-typed  $\text{ZnWO}_4$  (S.G.: P2/c; JCPDS No. 89-0447), respectively.

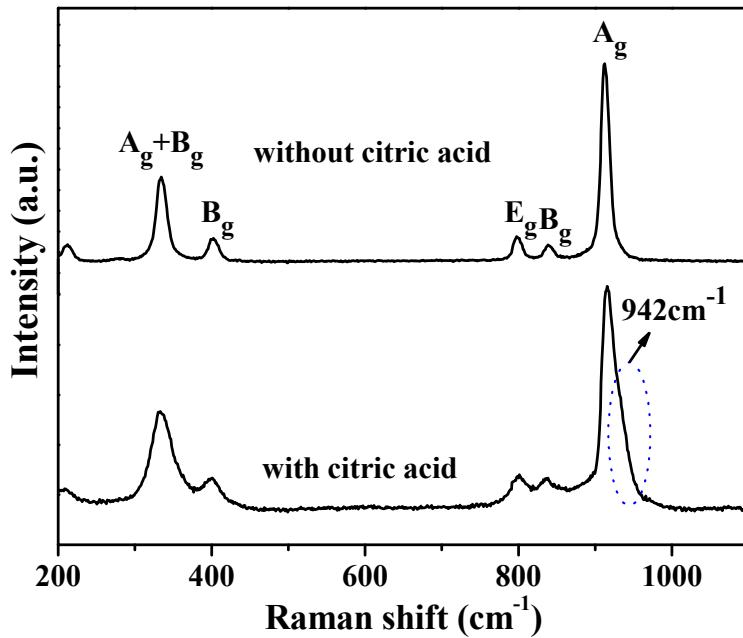


**Fig. S4.** Raman spectra of the samples prepared with and without involving citric acid. A shoulder centered at  $942\text{ cm}^{-1}$  was noticeably observed at the presence of citric acid, which cannot be ascribed to any vibrations of  $\text{CaWO}_4$  or other possible adsorbed species, but a new vibration of surface disordered layer as reported for  $\text{MnWO}_4$  nanocrystals<sup>ref\*</sup> prepared using the similar preparation conditions.

ref\*: W. M. Tong, L. P. Li, W. B. Hu, T. J. Yan, X. F. Guan and G. S. Li, *J. Phys. Chem. C*, 2010, **114**, 15298.

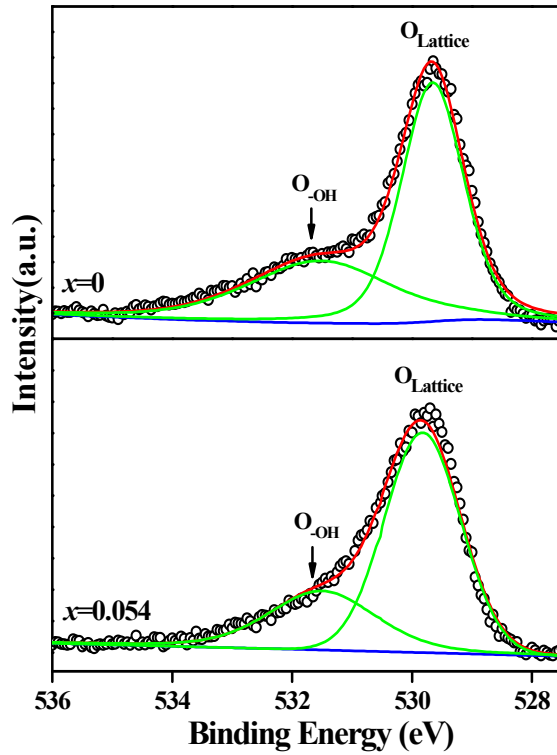


**Fig. S5.** High-resolution XPS spectra of O1s for  $\text{Ca}_{1-x}\text{Zn}_x\text{WO}_4$  nanocrystals at given dopant contents.

It is seen that the XPS data for both samples contained a dominant signal centered at 529.8 eV with a shoulder at 531.6 eV. The dominant signal is associated with the lattice oxygen, while the shoulder is originated from the adsorbed oxygen of the hydrated surfaces as indicated by TG data in Fig. 4.

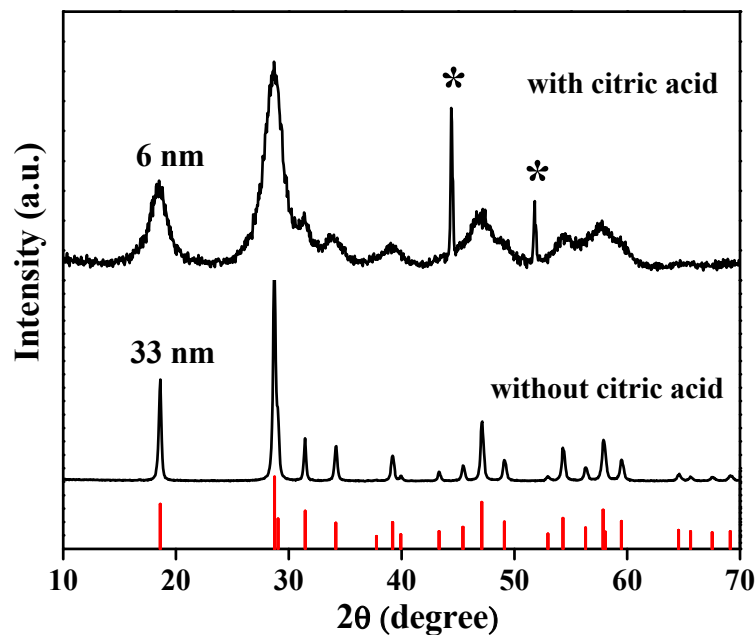


**Fig. S6.** XRD patterns of the samples prepared with and without involving citric acid. Vertical bars at the bottom denote the standard data for scheelite structure of bulk CaWO<sub>4</sub> (JCPDS, No. 77-2233). The average sizes were estimated to be 6 and 33 nm, which suggested that citric acid played an important role for the preparation of CaWO<sub>4</sub> nanocrystals.